Dynamical Bloch Band Suppression in an Optical Lattice

K. W. Madison, M. C. Fischer, R. B. Diener, Qian Niu, and M. G. Raizen
Department of Physics, The University of Texas at Austin, Austin, Texas 78712-1081
(Received 19 June 1998)

Dynamical Bloch band suppression is observed for the first time, using cold sodium atoms in a far detuned standing wave of light. This system has well-defined Bloch bands as its energy spectrum, which are modified dynamically by imposing a strong phase modulation of the standing wave. The atoms are prepared in the lowest band, and the spectrum is mapped out by introducing a weak spectroscopic probe that drives transitions between the modified bands. Dynamical suppression of the bands is observed at a critical value of the modulation strength, and is well supported by a full quantum mechanical analysis that goes beyond the single-band and tight-binding approximations. [S0031-9007(98)07857-0]

PACS numbers: 32.80.Pj, 42.50.Vk

Twelve years ago, Dunlap and Kenkre studied theoretically the problem of electron dynamics in a Bloch band driven by an ac electric field. They found the surprising result that dc transport of the electrons can be completely shut off when the strength of the ac field takes some special values [1]. This effect of dynamical localization was later found to be associated with a collapse of the Bloch bands in a Floquet analysis of the quasienergy spectrum by Holthaus [2]. These ideas reveal the possibility for a new and interesting solid state device, but their experimental realization has been difficult. The suppression of transport has indeed been observed on a superlattice driven by a terahertz free-electron laser [3], but it was interpreted as the inhibition of interwell tunneling rather than that of Bloch transport, because it is not clear if quantum coherence can be maintained over a distance of more than two wells.

In this Letter, we report the first observation of dynamical suppression of Bloch bands due to an ac field. Our system consists of laser-cooled atoms in an optical lattice, rather than electrons in a superlattice. The main advantage of our system is the long coherence times, limited only by residual spontaneous scattering. This feature has made it possible, in earlier work, to observe a number of important quantum phenomena such as Bloch oscillations, Wannier Stark ladders, and Landau-Zener tunneling [4]. In our experiments we trap neutral sodium atoms in the lowest band of a one-dimensional optical lattice. We then modulate the position of the potential to realize both an intense ac field and a weak spectroscopic probe in order to directly observe band suppression. The conceptual simplicity of the system enables a direct comparison with theory, and provides a new testing ground for the study of particle transport in this regime.

The optical lattice is a one-dimensional sinusoidal potential experienced by an atom in a standing wave of laser light. The light is detuned sufficiently far from resonance that spontaneous emission can be neglected, and the effective potential for the atom in its ground state is given by $V_0 \cos(2k_L x)$, where $k_L = 2\pi/\lambda_L$ is the photon wave number. The amplitude of this optical dipole potential V_0 is proportional to the laser intensity and inversely proportional to the detuning from the atomic resonance [5].

An ac field is added by imposing a phase modulation to one of the standing wave component fields. In the laboratory frame, the potential has the form $V_0 \cos[2k_L x - \lambda_s \sin(\omega_s t)]$, where λ_s and ω_s are the modulation index and frequency. In the comoving frame of the lattice, the Hamiltonian has the form

$$H_{\text{latt}} = \frac{p^2}{2M} + V_0 \cos(2k_L x) - x \frac{M\lambda_s\omega_s^2}{2k_L} \sin(\omega_s t), \tag{1}$$

where the mass of the atom M appears in the last term, revealing its inertial origin.

The eigenfunctions for this potential in the absence of the ac term are delocalized Bloch states and the distribution of energy levels is characterized by bands of allowed regions separated by band gaps. In the context of electronic motion in crystals under the influence of a driving laser field, it was shown that the dipole driving term modulates the bandwidths. In particular, the quasienergy band structure undergoes a dynamical suppression when $J_0(Fa/\hbar\omega_s) = 0$, where $F = M\lambda_s\omega_s^2/2k_L$ is the amplitude of the ac force, $a = \pi/k_L$ is the period of the lattice, and J_0 is the zeroth order Bessel function. In the tight-binding limit, where the well depth is large enough to consider only nearest-neighbor coupling, a full band collapse occurs in which the bandwidth shrinks to zero and the hitherto delocalized Bloch states become localized [1,2]. In this experiment, coupling to non-nearest neighbors as well as the presence of higher bands complicate the band evolution and prevent a complete collapse [6].

In order to observe the quasienergy band structure, we added a second phase modulation to the potential that was much weaker than the strong ac field. This weak probe did not significantly alter the quasienergy levels but could drive transitions between them. By preparing the atoms in the first band and measuring the depletion of its population as a function of the probe frequency, a spectrum was obtained.

The experimental setup for this spectroscopic study was based on the system used previously to study Wannier-Stark ladders and tunneling in optical lattices [7]. The optical standing wave was created by two linearly polarized, counterpropagating laser beams. The beams were spatially filtered to have a Gaussian profile with a waist of 2.0 mm at the location of the atomic cloud. The phase of the standing wave was controlled by adjusting the frequency difference of the component fields. The average power in each beam was 82 mW, and the instantaneous power for each run was monitored with two calibrated photodiodes. The detuning was chosen to be 32 GHz $\pm$ 100 MHz from the $(3S_{1/2}, F = 2) \leftrightarrow (3P_{3/2}, F = 3)$ transition at 589 nm. These parameters yielded a well depth of $V_0/h = 102$ kHz with an absolute uncertainty of $\pm 10\%$.

The preparation of a significant number of atoms in the lowest band of the optical lattice was achieved by using a magneto-optic trap (MOT) [8]. After the cooling and trapping stage, the MOT fields were extinguished and the optical lattice was turned on. Approximately 10% of our atoms were projected into the lowest band of the lattice. We then accelerated the lattice at $2\,000\ \mathrm{m/s^2}$ for 600 μs. This acceleration was chosen to maximize the tunneling out of the second and higher bands while minimizing losses from the first band. At the chosen acceleration and well depth, the Landau-Zener expression for the lifetimes of the first and second bands yields 18 s and 87 μs, respectively [9]. Therefore, only the first band was significantly bound to the potential during this acceleration, and the atoms occupying it were transported to a velocity of 1.2 m/s, separating them in velocity from the other atoms.

The acceleration was then stopped, and both the strong and weak phase modulations were turned on smoothly during 16 μs to avoid phase jumps which could drive transitions between bands. The total time that the atoms were exposed to the phase modulations was 500 μs. For each spectrum, the strong drive amplitude was fixed and the probe modulation frequency was scanned in the range 50–200 kHz. The modulation index of the weak probe was 0.05. In order that the strong drive only modify the band structure without driving transitions, its frequency was chosen to be $\omega_s/2\pi = 20$ kHz, far less than the width of the first band gap. To determine the depletion of the first band, an acceleration identical to the first was imposed to separate in velocity those atoms still in the first band from those which made transitions to higher states. After a 3 ms free drift, the resulting spatial distribution was "frozen" in place for 10 ms by an optical molasses; the fluorescence was imaged onto a charge-coupled-device camera. We resolved three groups of atoms which correspond to the MOT distribution left behind during the first acceleration, those atoms which were driven out of the first band during the modulation, and those atoms which survived the modulation and were accelerated to the final velocity. The fraction remaining in the first band was obtained by normalizing the number of survivors by the total number of atoms initially trapped.

Figure 1 shows a series of measured spectra for increasing ac field strengths. When there is no strong field present ($\lambda_s = 0$) we obtain a spectrum of the unperturbed Bloch band structure (Fig. 1a). Although the spectrum maps the transition from the first to second band ($1 \leftrightarrow 2$), the spectrum width represents that of the second band since, for the chosen well depth, the first band is only 3 kHz wide which is small compared to the 32 kHz width of the second band. As the modulation strength is increased, the second band flattens and side peaks spaced at multiples of the strong field frequency grow in size. For a modulation index of $\lambda_s = 3.8$, the condition for band collapse is fulfilled. For this case, the central peak is at its narrowest with a half-width of approximately 15 kHz. As the modulation index is increased past the band collapse condition, the central peak broadens and the previously distinct side peaks overlap, producing broad tails on the central resonance.

Mirror vibration and frequency instabilities of our electronic drivers caused a low frequency fluctuation of the standing wave position which excited atoms out of the lowest band at a constant rate. This loss, which was constant for each run, resulted in a background of lost atoms and

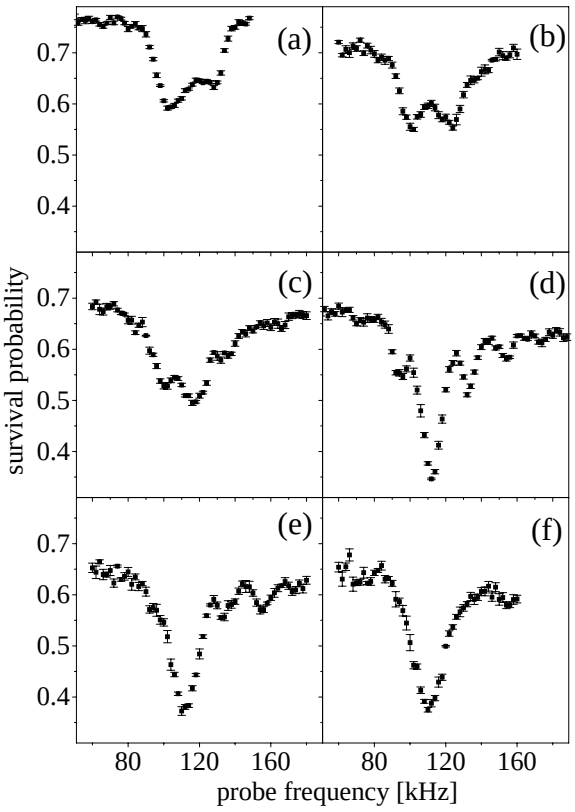

FIG. 1. Measured survival probability in the lowest band as a function of probe frequency for six different strong field modulation strengths. In (a)–(f) the values for λ_s were 0, 1, 2, 3.8, 4.3, and 5, respectively. Spectrum (a) is of the unperturbed Bloch band, and spectrum (d) is of the system at the band collapse condition. The side peaks which develop are separated by the strong ac modulation frequency (20 kHz) and correspond to multiphoton transitions. Each point is an average of several runs and the error bar denotes the one-sigma error of the mean.

prevented the survival probability from approaching unity even when the probe was far from resonance. An additional complication arose from the fact that although the strong ac modulation frequency was far from resonance for the $(1 \leftrightarrow 2)$ transition, its amplitude was nevertheless large enough to drive off-resonant transitions. This explains the drop of the base line for larger values of λ_s.

In the theoretical analysis of this problem we calculated the quasienergies and their corresponding coupling strengths between the first and higher bands in order to generate a prediction for the experimental spectral distributions of Fig. 1. For convenience, we used scaled units, in which $\hbar = M = 2k_L = 1$. In these units, the frequency and well depth scale as $\omega_s \rightarrow \omega_s/8\omega_r$ and $V_0 \rightarrow V_0/8\hbar\omega_r$, where $\omega_r = 2\pi \times 25$ kHz is the single photon recoil frequency. A unitary transformation of the Hamiltonian in Eq. (1) yields

$$H_0 = \frac{[p - \lambda_s \omega_s \cos(\omega_s t)]^2}{2} + V_0 \cos(x). \qquad (2)$$

The Hamiltonian is periodic in both time and space with periods $T = 2\pi/\omega_s$ and 2π, respectively. Floquet's theorem shows that states exist of the form $\Psi_{\epsilon,k}(x,t) = e^{i(kx-\epsilon t)} u_{\epsilon,k}(x,t)$ with $u_{\epsilon,k}(x,t+T) = u_{\epsilon,k}(x,t) = u_{\epsilon,k}(x+2\pi,t)$ which satisfy $H_0\Psi_{\epsilon,k} = i\dot{\Psi}_{\epsilon,k}$. In analogy with the time-independent case, ϵ is called the quasienergy of the state and is defined up to an integer multiple of the frequency ω_s. It is also periodic in the lattice momentum k which is conventionally restricted to the first Brillouin zone, the interval $(-1/2, 1/2]$.

The problem of finding the quasienergies and their associated vectors can be solved in the following manner. First, write the wave function as $\Psi_{\epsilon,k}(x,t) = e^{i(kx-\epsilon t)} \times \sum_{n,m} c_{n,m} e^{i(nx - m\omega_s t)}$ and insert this expression into Schrödinger's equation. Second, solve the set of equations obtained for the coefficients $c_{n,m}$ and the quasienergy ϵ. The most general representation of the spectrum is the repeated-zone scheme in which each quasienergy is represented by all of its possible values $\epsilon + j\omega_s$, for integer values of j.

Transitions from the first to higher bands were achieved, as in the experiment, by introducing a second, weak ac field of frequency ω. The Hamiltonian can be written as $H(t) = H_0(t) - p\lambda\omega \cos(\omega t)$, where $H_0(t)$ is given by Eq. (2) and $\lambda \ll \lambda_s$. k is still a conserved quantity since the new term is a small perturbation which preserves the lattice periodicity.

Assume that an atom is in the quasienergy state $\Psi_{\epsilon_1,k} = |1\rangle$ corresponding to the first band and that the perturbation only drives transitions to one other quasienergy state $\Psi_{\epsilon_2,k} = |2\rangle$ (this approximation is valid as long as the frequency ω is close to resonance). Given the state vector of the atom, $\Psi = a_1|1\rangle + a_2|2\rangle$, the equations of motion for a_1 and a_2 are

$$i\dot{a}_1 = -\lambda\omega \cos(\omega t)[a_1\langle 1|p|1\rangle + a_2\langle 1|p|2\rangle], \qquad (3a)$$

$$i\dot{a}_2 = -\lambda\omega \cos(\omega t)[a_1\langle 2|p|1\rangle + a_2\langle 2|p|2\rangle]. \qquad (3b)$$

For short times the second state is not significantly populated, so that $|a_2| \ll |a_1| \approx 1$. To lowest order, $\dot{a}_2 = i\lambda\omega \cos(\omega t)\langle 2|p|1\rangle$. Since the quasienergy states are not stationary, the time dependence of the matrix element $\langle 2|p|1\rangle$ contains many frequencies:

$$e^{\pm i\omega t}\langle 2|p|1\rangle = \sum_j e^{i(\epsilon_2 - \epsilon_1 + j\omega_s \pm \omega)t} \Gamma_j(k), \qquad (4)$$

where $\Gamma_j(k) = \sum_{n,m}(k+n) c^{(1)}_{n,m} (c^{(2)}_{n,m+j})^*$. Resonant transitions occur whenever $\epsilon_2 - \epsilon_1 \approx \pm\omega - j_0\omega_s$ for some value of j_0. These are multiphoton transitions in which $|j_0|$ is the number of participating photons of the strong field. In analogy with the rotating wave approximation where only the resonant term is kept, we approximated Eq. (4) by just one term of the sum,

$$e^{\pm i\omega t}\langle 2|p|1\rangle = e^{i(\epsilon_2 - \epsilon_1 + j_0\omega_s \pm \omega)t} \Gamma_{j_0}(k). \qquad (5)$$

We are keeping the term in Eq. (3) with the slowest temporal dependence. All other terms will produce fast population oscillations with frequencies of integer multiples of ω_s. In the presence of strong resonances, they do not contribute appreciably to the measured transition probabilities.

The quasienergies were calculated numerically for the cases in which $\lambda_s = 0$, 3.8, and 5.2. The values $\omega_s = 0.10$ and $V_0 = 0.510$, corresponding to $\omega_s/2\pi = 20$ kHz and $V_0/h = 102$ kHz in real units, were chosen to match the parameters used in the experiment. The results are shown in the left panel of Fig. 2 in scaled units. The lowest band, located at about -0.2, is not shown in the figure. The results were plotted in the repeated-zone scheme in quasienergy space and in the restricted-zone scheme in k space. The three values of λ_s chosen correspond to (a) no strong ac field, (b) at, and (c) past the condition for band collapse. The plot of $\epsilon_2(k) + j_0\omega_s$ was gray scaled by the value of $[\Gamma_{j_0}(k)]^2$ which determines the transition probability and therefore the quasienergies that are important.

When $\lambda_s = 0$ the quasienergy spectrum is simply the real energy spectrum repeated with periodicity ω_s. However, only one representation of each quasienergy is present in Fig. 2a since all values of $\Gamma_{j_0}(k)$ with $j_0 \neq 0$ are zero. This is due to the absence of photons with frequency ω_s, which are necessary for such transitions. The plot shows the second band and part of the third band. As λ_s is increased, multiphoton transitions become more probable and some of the repetitions of the bands become visible. The repetitions of the original second and third bands interact and develop avoided level crossings.

The effect of a strong ac electric field on a single band has been studied previously [2]. In this model, the coupling between the different Bloch bands is not taken into account. For comparison, the second band was calculated using this model and the results were plotted with dashed lines. For the band collapse condition (Fig. 2b) this model predicts an almost flat band. However, the Floquet analysis shows that the avoided crossings significantly broaden

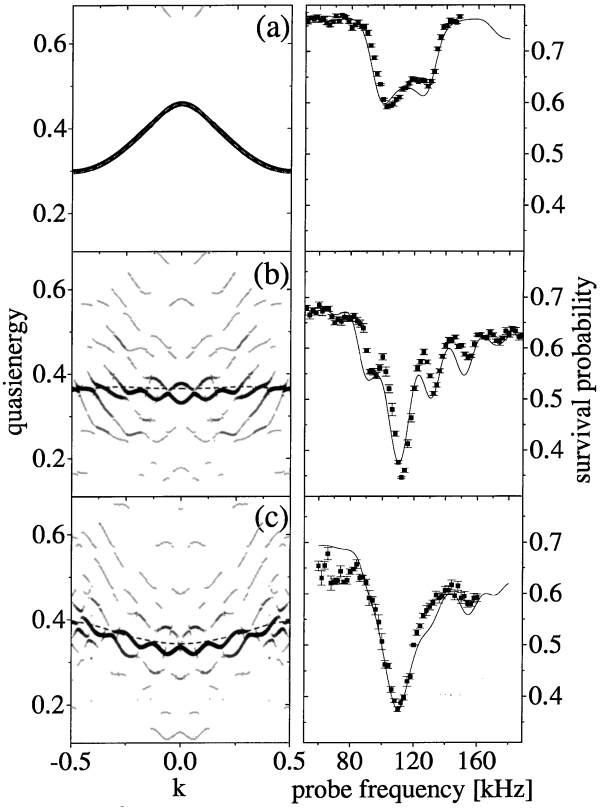

FIG. 2. The left three panels are plots of the calculated quasienergies versus k for three values of λ_s (0, 3.8, and 5.2) in scaled units. We restricted our attention to the energy range [0.1, 0.7] which corresponds to energies accessed by our probe. In addition, the quasienergies were plotted using a gray scale to differentiate their on-resonant coupling strengths $\Gamma_{j_0}(k)$. For comparison, the single-band approximation result is shown by the dashed line. To the right of each panel is the experimentally measured spectrum (points with error bars) and the theoretical spectrum (thin line) predicted from the calculated quasienergy bands.

the bandwidth beyond the predictions of the single-band model.

Using the calculated quasienergies and their corresponding matrix elements, we generated spectral distributions to compare with the experimental data. Rabi oscillations are known to govern the transition probabilities between bands and have been characterized in this system [10]. In order to calculate the survival probability for the first band as a function of ω, we used the approximation Eq. (5) and neglected the diagonal terms in Eq. (3) (the weak probe drives transitions between bands but does not change their shape or position). The results shown in the right panels of Fig. 2 were obtained by assuming that the first band was uniformly populated. In addition, the spectra were averaged to account for the finite Gaussian bandwidth of the weak probe used in the experiment. There were two additional experimental effects which had to be accounted for in order to compare the spectral distributions. The first effect, mentioned previously, was a base line shift due to a constant loss of atoms from the optical lattice. The second was a systematic underestimate of the survival probability due to nonuniform detection of our atomic sample. The spectra were scaled and the base lines shifted to compensate for these effects. The absolute position and shape of the resonances, which are the most important features, are independent of these effects. The agreement between the measured and calculated spectra is good, indicating that the approximation in Eq. (5) is valid and that Fig. 2 is a faithful representation not only of the quasienergies but also of their respective coupling strength with the lowest band.

In summary, we have observed dynamical Bloch band suppression in a system of cold sodium atoms in an optical lattice in the presence of a strong ac field. These results are in good agreement with a full quantum mechanical analysis of the problem, which goes beyond the tight-binding and single-band approximations. In the future, we plan to investigate the role of decoherence on band collapse, and to extend these measurements to a many body atomic system.

This work was supported by the R. A. Welch Foundation and the National Science Foundation.

[1] D. H. Dunlap and V. M. Kenkre, Phys. Rev. B **34**, 3625 (1986).
[2] M. Holthaus, Phys. Rev. Lett. **69**, 351 (1992); X.-G. Zhao, J. Phys. **6**, 2751 (1994); K. Drese and M. Holthaus, Chem. Phys. **217**, 201 (1997).
[3] B. J. Keay, S. Zeuner, S. J. Allen, Jr., K. D. Maranowski, A. C. Gossard, U. Bhattacharya, and M. J. W. Rodwell, Phys. Rev. Lett. **75**, 4102 (1995).
[4] M. G. Raizen, C. Salomon, and Q. Niu, Phys. Today **50(7)**, 30 (1997).
[5] C. Cohen-Tannoudji, in *Les Houches, Session LIII, 1990—Fundamental Systems in Quantum Optics*, edited by J. Dalibard, J. M. Raimond, and J. Zinn-Justin (Elsevier, New York, 1992).
[6] X.-G. Zhao and Q. Niu, Phys. Lett. A **222**, 435 (1996).
[7] S. R. Wilkinson, C. F. Bharucha, K. W. Madison, Q. Niu, and M. G. Raizen, Phys. Rev. Lett. **76**, 4512 (1996); C. F. Bharucha, K. W. Madison, P. R. Morrow, S. R. Wilkinson, B. Sundaram, and M. G. Raizen, Phys. Rev. A **55**, R857 (1997); S. R. Wilkinson, C. F. Bharucha, M. C. Fischer, K. W. Madison, P. R. Morrow, Q. Niu, B. Sundaram, and M. G. Raizen, Nature (London) **387**, 575 (1997).
[8] Steven Chu, Science **253**, 861 (1991).
[9] Q. Niu, X.-G. Zhao, G. A. Georgakis, and M. G. Raizen, Phys. Rev. Lett. **76**, 4504 (1996).
[10] M. C. Fischer, K. W. Madison, Qian Niu, and M. G. Raizen, Phys. Rev. A **58**, R2648 (1998).